

Fast expectation-maximization algorithms for spatial generalized linear mixed models

Yawen Guan¹ and Murali Haran²

¹Department of Statistics, University of Nebraska,

Email: yguan12@unl.edu

²Department of Statistics, Pennsylvania State University,

Email: mharan@stat.psu.edu

Abstract

Spatial generalized linear mixed models (SGLMMs) are popular and flexible models for non-Gaussian spatial data. They are useful for spatial interpolations as well as for fitting regression models that account for spatial dependence, and are commonly used in many disciplines such as epidemiology, atmospheric science, and sociology. Inference for SGLMMs is typically carried out under the Bayesian framework at least in part because computational issues make maximum likelihood estimation challenging, especially when high-dimensional spatial data are involved. Here we provide a computationally efficient projection-based maximum likelihood approach and two computationally efficient algorithms for routinely fitting SGLMMs. The two algorithms proposed are both variants of expectation maximization (EM) algorithm, using either Markov chain Monte Carlo or a Laplace approximation for the conditional expectation. Our methodology is general and applies to both discrete-domain (Gaussian Markov random field) as well as continuous-domain (Gaussian process) spatial models. Our methods are also able to adjust for spatial confounding issues that often lead to problems with interpreting regression coefficients. We show, via simulation and real data applications, that our methods perform well both in terms of parameter estimation as well as prediction. Crucially, our methodology is computationally efficient and scales well with the size of the data and is applicable to problems where maximum likelihood estimation was previously infeasible.

Key words: Laplace approximation, Markov chain Monte Carlo expectation maximization, Projection-based models, Non-Gaussian.

1 Introduction

Non-Gaussian spatial data arise in a number of disciplines, for instance when modeling disease incidence in epidemiology (see, for example Diggle et al., 1998; Hughes and Haran, 2013) or modeling weed counts and plant disease in agriculture (Christensen and Waagepetersen, 2002; Zhang, 2002). Spatial generalized linear mixed models (SGLMMs) are convenient and flexible models for such data. Following two seminal papers, Diggle et al. (1998) and Besag et al. (1991), SGLMMs have been very popular, not only in mainstream statistics but also in many other disciplines. These models are useful both for data observed on a continuous spatial domain such as at irregularly-positioned sampling locations and data observed on a discrete spatial domain such as county-level data. In this manuscript, we propose two fast maximum likelihood (ML) inference algorithms for a projection-based approach that are applicable for both the continuous and discrete spatial domains.

Inference for SGLMMs is commonly carried out under the Bayesian paradigm (see Banerjee et al., 2014; Haran, 2011). However, constructing efficient Markov Chain Monte Carlo (MCMC) samplers for fitting such models to large data sets is often challenging. There are two major computational challenges: (1) computational issues due to high-dimensional random effects that are typically heavily cross-correlated – these often result in slow mixing Markov chain Monte Carlo algorithms; (2) expensive calculations involving large matrices. An additional issue is spatial confounding between fixed and random effects – this can result in slow mixing and problems with parameter interpretation (cf. Guan and Haran, 2018; Reich et al., 2006; Hanks et al., 2015; Hughes and Haran, 2013). Under a Bayesian framework, the high-dimensional computational challenges for SGLMMs have been addressed via the predictive process approach (Banerjee et al., 2008) and the Vecchia-Laplace approximation (Zilber and Katzfuss, 2021), the MCMC mixing issues have been addressed by various reparameterizations (cf. Christensen et al., 2006; Haran et al., 2003; Rue and Held, 2005), and the confounding issues have been addressed in Reich et al. (2006). Rue et al. (2009) provided a fast inferential approach based on nested Laplace approximations and Lindgren et al. (2011) suggested how this approximation may be adapted to continuous spatial domain SGLMMs. Recently, via projection-based methods, Hughes and Haran (2013) and Guan and Haran

(2018) have addressed both the above computational as well as confounding issues within a Bayesian approach.

We consider ML inference for SGLMMs, which had received less attention, at least in part, because of computational challenges. For data sets with just a few hundred data points, a Monte Carlo EM (MCEM) algorithm (Zhang, 2002) and a Monte Carlo maximum likelihood (MCML) algorithm (Christensen, 2004) were proposed for fitting SGLMMs. However, neither algorithm extends easily to large data sets because they both require simulation of the high-dimensional latent variables, which is computationally expensive when the data sets are large. Sengupta and Cressie (2013b,a) developed fast ML inference for large non-Gaussian observations by approximating the spatial random effects with basis functions to resolve computational issues. The projection-based methods used in this manuscript (Hughes and Haran, 2013; Guan and Haran, 2018) can be thought of as a fixed-rank approach, but use data driven basis functions. More recently, Park and Haran (2020) develop a Monte Carlo maximum-likelihood (MCML) algorithm for fitting SGLMMs. This approach is able to handle higher dimensional problems than previously considered. However, MCML algorithms can be challenging to implement for non-experts. The EM algorithms we propose in this paper, particularly the Laplace approximation-based version, are generally easier to implement than MCMLE. Furthermore, after the seminal paper by Zhang (2002) on EM for SGLMMs, there has been relatively little if any work on EM algorithms for the kind of generalized linear models with high-dimensional dependent latent variables that we consider in this manuscript. To our knowledge, the algorithms here are therefore among the first viable EM algorithms for such models for large data sets: our approach for using a projection-based dimension reduction of the latent variables opens up interesting new avenues for developing EM algorithms that are practical for such models. Bonat and Ribeiro (2016) developed an approximate likelihood-based approach, which substitutes a Laplace approximation for Monte Carlo simulation. However, it is unclear how well this approach will work for high-dimensional problems as it requires Gaussian approximations to the full conditional distribution of high-dimensional latent variable.

Our contribution in this manuscript is to provide computationally efficient ML inference for SGLMMs for large data with the ability to address spatial confounding. We develop two

variants of the expectation maximization (EM) algorithm, Markov chain Monte Carlo EM (MCMC-EM) and Laplace approximation EM (LA-EM), for maximum likelihood estimation. Our approach provides the ability to fit SGLMMs routinely by (i) having an automated algorithm for estimation, (ii) reducing the computational cost of the estimation algorithm, (iii) addressing spatial confounding issues, and (iv) sidestepping the need to provide hyperpriors for parameters about which there is often little available information. Our manuscript also contributes to the study of practical issues in constructing MCMC-EM algorithms in the context of a challenging latent variable model. We believe, as applied statisticians ourselves, that the above characteristics are useful to researchers who use SGLMMs in applications. For problems that involve fitting an SGLMM to a spatial data set in more complicated settings where an additional hierarchy in the modeling framework becomes necessary, for instance where multiple data sets need to be integrated, we would likely revert to a Bayesian approach.

The outline of the remainder of the paper is as follows. In Section 2, we describe SGLMMs and spatial confounding. We introduce in Section 3 the projection-based SGLMMs and in Section 4 the MCMC-EM and LA-EM algorithms for ML inference. We study our method via a simulation study in Section 5 and apply it to two data sets in Section 6. We conclude with a discussion and potential areas for future work in Section 7.

2 Spatial Generalized Linear Mixed Models

2.1 Models

SGLMMs provide a framework for analyzing spatially dependent non-Gaussian observations. Let $Z(\mathbf{s})$ denote the response variable, $\mathbf{x}(\mathbf{s}) = (x_1(\mathbf{s}), \dots, x_p(\mathbf{s}))^T$ denote the explanatory variables, and $W(\mathbf{s})$ represent a spatial random field, where $\mathbf{s} \in \mathbb{R}^2$ indicates a spatial location. For data obtained at a finite collection of locations $\mathcal{S} = \{\mathbf{s}_1, \dots, \mathbf{s}_n\}$, we write $Z_i = Z(\mathbf{s}_i)$ and let $\mathbf{Z} = (Z_1, \dots, Z_n)^T$ be a vector of the observed response variable at \mathcal{S} . Similarly, let $\mathbf{X} = (\mathbf{x}_1, \dots, \mathbf{x}_n)$ and $\mathbf{W} = (W_1, \dots, W_n)^T$ be the corresponding finite counterparts. The SGLMMs can be defined with three components.

(i) A model for spatial random effects. This can change depending on whether the data are on a discrete (lattice) or continuous spatial domain. For a continuous spatial domain, $W(\mathbf{s})$ is often modeled as a zero-mean stationary Gaussian random field with $\text{cov}(W(\mathbf{s}), W(\mathbf{s}')) = C(\|\mathbf{s} - \mathbf{s}'\|)$ for $\mathbf{s}, \mathbf{s}' \in \mathcal{R}^2$, where the covariance function $C(\cdot)$ depends on a vector of parameters $\boldsymbol{\theta}$. Hence, \mathbf{W} follows a multivariate normal distribution, $f(\mathbf{W}|\boldsymbol{\theta}) \propto |\Sigma_{\boldsymbol{\theta}}|^{-1/2} \exp\left(-\frac{1}{2}\mathbf{W}^T \Sigma_{\boldsymbol{\theta}}^{-1} \mathbf{W}\right)$. A frequently used covariance function, assuming stationarity and isotropy, is the Matérn class (Stein, 1999). For a discrete spatial domain, \mathbf{W} is typically modeled as a zero-mean Markov random field. The index of W_i indicates a node on a lattice, typically denoting a geographic block. The neighboring structure among blocks is defined through an $n \times n$ adjacency matrix A , with $\text{diag}(A) = 0$ and $A_{ij} = 1$ if the i^{th} and j^{th} locations are connected (Besag et al., 1991). A popular model for \mathbf{W} is the intrinsic conditionally auto-regressive (ICAR) model, $f(\mathbf{W}|\tau) \propto \tau^{\text{rank}(Q)/2} \exp\left(-\frac{\tau}{2}\mathbf{W}^T Q \mathbf{W}\right)$, where τ is a parameter that controls the smoothness of the spatial field and $Q = \text{diag}(A\mathbf{1}) - A$ is the precision matrix, and $\mathbf{1}$ is an n -dimensional vector of ones.

(ii) Conditional on \mathbf{W} and $\boldsymbol{\beta}$, observations \mathbf{Z} are independently distributed with distribution function $\prod_{i=1}^n f_{Z_i|W_i}(Z_i|W_i, \boldsymbol{\beta})$. Each observation has a site-specific conditional mean $\mu_i = E[Z_i|W_i, \boldsymbol{\beta}]$.

(iii) A link function g that relates the conditional mean to a linear model, $g(\mu_i) = \mathbf{x}_i^T \boldsymbol{\beta} + W_i$. For instance, it is common to use a log link for counts.

In the remaining sections, we use $\boldsymbol{\theta}$ to denote parameters of the spatial random fields for both continuous and discrete cases to unify the notations, although $\boldsymbol{\theta}$ is a scalar in the latter case. The observed-data likelihood or SGLMMs has the form

$$L(\boldsymbol{\beta}, \boldsymbol{\theta}; \mathbf{Z}) = \int_{\mathbb{R}^n} \left\{ \prod_{i=1}^n f_{Z_i|W_i}(Z_i|W_i, \boldsymbol{\beta}) \right\} f_{\mathbf{W}}(\mathbf{W}|\boldsymbol{\theta}) d\mathbf{W}, \quad (1)$$

which involves a high-dimensional integral and is typically not available in closed form. Therefore, direct maximization of (1) is infeasible. Monte Carlo maximum likelihood (Geyer and Thompson 1992) and Monte Carlo versions of EM algorithms (cf., Wei and Tanner 1990, McCulloch 1994) have been proposed to approximate the integration in (1) using Monte Carlo samples (Christensen, 2004; Zhang, 2002). These Monte Carlo methods require simulations

from the conditional distribution of random effects given the data, $f_{\mathbf{W}}(\mathbf{W}|\boldsymbol{\theta}, \mathbf{Z})$, for both inference and prediction. These methods work quite well for data sets that are relatively small, say in the hundreds. When confronted with thousands of data points or more, these methods become computationally challenging. This is largely because, like in the Bayesian approach, the number of random effects grows with the size of the data. This results in a high-dimensional integration problem at each iteration of the EM algorithm which, in turn, leads to an unstable MCMC-EM algorithm. Furthermore, it becomes difficult to construct a fast mixing MCMC algorithm at each expectation step because the random effects are often highly cross-correlated. In addition to addressing these challenges via the projection-based approach, we provide some guidance on how to tune the algorithm, including, for instance, how to determine appropriate Monte Carlo sample sizes for each step of the algorithm.

2.2 Spatial Confounding

Let $P_{[X]} = X(X^T X)^{-1}X^T$ and $P_{[X]}^\perp = I - P_{[X]}$ denote the orthogonal projections onto the span of X and its complement, respectively. The confounding problem therefore arises in much the same way as in multicollinearity problems with standard regression models. The only difference here is that the confounding arises because of the spatial random effects. The linear model for cite-specific conditional means, $\boldsymbol{\mu} = (\mu_1, \dots, \mu_n)^T$, is $g(\boldsymbol{\mu}) = X\boldsymbol{\beta} + \mathbf{W} = X\boldsymbol{\beta} + P_{[X]}\mathbf{W} + P_{[X]}^\perp\mathbf{W}$. Since $P_{[X]}\mathbf{W}$ is confounded with X , Hodges and Reich (2010) suggested that it should be removed from the model to alleviate spatial confounding. However, Hanks et al. (2015) argues that when $P_{[X]}\mathbf{W}$ is “removed” from the model, its effect is combined with $\boldsymbol{\beta}$ and an *a posteriori* adjustment should be performed to obtain valid inference about $\boldsymbol{\beta}$. This way of restricting the random effects to be orthogonal to the fixed effects is also called restricted spatial regression (RSR) model. Methods for addressing these problems have been developed and studied for both continuous and discrete domain data (cf. Reich et al., 2006; Hanks et al., 2015; Guan and Haran, 2018; Hughes and Haran, 2013).

3 A Projection-Based Approach to Dimension Reduction

To address the computational and confounding issues, we consider two projection-based models for the continuous and discrete spatial domains (Guan and Haran, 2018; Hughes and Haran, 2013). Both models leverage efficient reparameterizations to (1) reduce the dimension of the random effects and (2) alleviate spatial confounding. They share a common form, $P_{[X]}^\perp \mathbf{W} \approx M\boldsymbol{\delta}$, where $\boldsymbol{\delta}$ is an m -dimensional vector with nearly independent elements and M is an $n \times m$ projection matrix that preserves the spatial information of \mathbf{W} . The projection matrix for the continuous case is computed based on the covariance matrix driven by the data, while for the discrete case it is based on the graph based on the neighboring structure.

For continuous case, an example is $C(h) = \sigma^2(1 + \sqrt{3}h/\phi) \exp(-\sqrt{3}h/\phi)$, which corresponds to the Matérn with smoothness $\nu = 1.5$ and $\boldsymbol{\theta} = (\sigma^2, \phi)^T$. Let R_ϕ denote the correlation matrix of \mathbf{W} and $\Sigma_\theta = \sigma^2 R_\phi$. Guan and Haran (2018) proposed to reparameterize \mathbf{W} using the first $m (<< n)$ principal component of R_ϕ and then project the reduced-dimensional random effects to the orthogonal span of X . Let $U_\phi = [\mathbf{u}_1, \dots, \mathbf{u}_m]$ denote the first m eigenvectors and $D_\phi = \text{diag}(\lambda_1, \dots, \lambda_m)$ a diagonal matrix containing eigenvalues of R_ϕ . The reparameterized random effects have the form $\widetilde{\mathbf{W}} = U_\phi D_\phi^{1/2} \boldsymbol{\delta}$, which result in independent random effects $\boldsymbol{\delta} | \sigma^2, \phi \sim N(0, \sigma^2 I)$, and $P_{[X]}^\perp \widetilde{\mathbf{W}} = M_\phi \boldsymbol{\delta}$, where $M_\phi = P_{[X]}^\perp U_\phi D_\phi^{1/2}$, is restricted to be orthogonal to the fixed effects. The hierarchical model becomes

$$g\{E[\mathbf{Z}|\boldsymbol{\beta}, M_\phi, \boldsymbol{\delta}]\} = X\boldsymbol{\beta} + M_\phi \boldsymbol{\delta}, \quad \boldsymbol{\delta} | \sigma^2, \phi \sim N(\mathbf{0}, \sigma^2 I).$$

If exact eigendecomposition is computationally infeasible, say when there are several thousands of data points, we can approximate it using a probabilistic version of the Nyström's method. An outline of the approximation algorithm is presented in the supplementary materials; details are provided in Guan and Haran (2018); Banerjee et al. (2013).

For discrete case, the reparameterization is based on the first m principal components, M_A , of the Moran operator $P^\perp A P^\perp$ (Hughes and Haran, 2013). The model has the form $g\{E[\mathbf{Z}|\boldsymbol{\beta}, \boldsymbol{\delta}]\} = X\boldsymbol{\beta} + M_A \boldsymbol{\delta}$, $p(\boldsymbol{\delta}|\tau) \propto \tau^{q/2} \exp(-\frac{\tau}{2} \boldsymbol{\delta}^T Q_\delta \boldsymbol{\delta})$, where $Q_\delta = M_A^T Q M_A$.

4 ML Inference Methods

Two variants of the EM algorithm are derived here for fitting the projection-based models. The EM algorithm iterates between the expectation step (E-step) and maximization step (M-step) for parameter estimation. The two EM variants proposed here are distinct in their approximations to the conditional expectation in the E-step; one uses Monte Carlo averages and the other uses a Laplace approximation.

The projection-based model facilitates fast ML inference because its observed-data likelihood has a much smaller dimension integration compared to the full model (1),

$$L(\boldsymbol{\beta}, \boldsymbol{\theta}; \mathbf{Z}) = \int_{\mathbb{R}^m} \left\{ \prod_{i=1}^n f_{Z_i|M\boldsymbol{\delta}}(Z_i|M\boldsymbol{\delta}, \boldsymbol{\beta}) \right\} f_{\boldsymbol{\delta}}(\boldsymbol{\delta}|\boldsymbol{\theta}) d\boldsymbol{\delta}. \quad (2)$$

For instance, in our simulation study $m = 50$ is sufficient for a data size of 1,000 in some settings, based on the rank selection guidelines provided in Section 4.4; moreover, $\boldsymbol{\delta}$ is less correlated than the original random effects. The reduced-dimensional and de-correlated random effects make it easier to construct a sampling algorithm (Section 4.2). The reparameterization also reduces matrix operation cost for Laplace approximation (Section 4.3).

4.1 Projection-Based EM

The projection-based EM algorithm is outlined here, and details for the two proposed EM variants are presented in the subsequent sections. For ease of representation, we write $\boldsymbol{\psi} = (\boldsymbol{\beta}, \boldsymbol{\theta})$ and let $f_{Z,\boldsymbol{\delta}}(\mathbf{Z}, \boldsymbol{\delta}; \boldsymbol{\psi})$ denote the integrand in (2). In an EM algorithm, random effects $\boldsymbol{\delta}$ are treated as missing data and $f_{Z,\boldsymbol{\delta}}(\mathbf{Z}, \boldsymbol{\delta}; \boldsymbol{\psi})$ is called the complete-data likelihood.

Let $\boldsymbol{\psi}^{(t)}$ be the current estimate of the ML estimator (MLE) $\hat{\boldsymbol{\psi}}$. The EM algorithm iterates between the following two steps for $t = 1, 2, 3, \dots$,

E-step: compute $Q(\boldsymbol{\psi}, \boldsymbol{\psi}^{(t)}) = E[\ln f_{Z,\boldsymbol{\delta}}(\mathbf{Z}, \boldsymbol{\delta}; \boldsymbol{\psi}) | \mathbf{Z}, \boldsymbol{\psi}^{(t)}]$ under $\boldsymbol{\psi}^{(t)}$,

M-step: find $\boldsymbol{\psi}^{(t+1)}$ to satisfy $Q(\boldsymbol{\psi}^{(t+1)}, \boldsymbol{\psi}^{(t)}) \geq Q(\boldsymbol{\psi}^{(t)}, \boldsymbol{\psi}^{(t)})$,

until the pre-specified stopping criterion are reached. The stopping rule is similar to the framework of determining Monte Carlo sample sizes based on the ascent-based approach

(Caffo et al., 2005); details are provided in the supplementary materials. Under some regularity conditions, the EM sequence converges to the unique MLE (Wu, 1983).

We use a gradient approach for obtaining $\boldsymbol{\psi}^{(t+1)}$ in the M-step, where a one-step Newton-Raphson replaces the maximization. This EM gradient algorithm speeds up EM convergence and is proven to be useful in the classical settings (cf. Lange, 1995); it was later extended to fitting SGLMMs (Zhang, 2002) for problems where the data size is relatively small. To maximize $Q(\boldsymbol{\psi}, \boldsymbol{\psi}^{(t)})$, we find its first and second derivative, Q' and Q'' , with respect to $\boldsymbol{\psi}$, then update the parameters using $\boldsymbol{\psi}^{(t+1)} = \boldsymbol{\psi}^{(t)} - Q''(\boldsymbol{\psi}^{(t)})^{-1}Q'(\boldsymbol{\psi}^{(t)})$. When the derivatives, $\partial/\partial\boldsymbol{\psi} \ln f_{\mathbf{Z},\delta}(\mathbf{Z}, \boldsymbol{\delta}; \boldsymbol{\psi})$ and $\partial^2/\partial\boldsymbol{\psi}\partial\boldsymbol{\psi}^T \ln f_{\mathbf{Z},\delta}(\mathbf{Z}, \boldsymbol{\delta}; \boldsymbol{\psi})$, are available in closed form, their respective conditional expectations,

$$\begin{aligned} Q' &= E \left[\frac{\partial}{\partial\boldsymbol{\psi}} \ln f_{\mathbf{Z},\delta}(\mathbf{Z}, \boldsymbol{\delta}; \boldsymbol{\psi}) | \mathbf{Z}, \boldsymbol{\psi}^{(t)} \right], \\ Q'' &= E \left[\frac{\partial^2}{\partial\boldsymbol{\psi}\partial\boldsymbol{\psi}^T} \ln f_{\mathbf{Z},\delta}(\mathbf{Z}, \boldsymbol{\delta}; \boldsymbol{\psi}) | \mathbf{Z}, \boldsymbol{\psi}^{(t)} \right], \end{aligned} \tag{3}$$

can be approximated using Monte Carlo samples or a Laplace approximation. For the projection-based models in Section 3, we have closed form expressions of the derivatives for all parameters except the range parameter (in the continuous case), and Q'' is block diagonal. The latter results in separate updating equations for the regression and spatial parameters.

Estimation for $\boldsymbol{\beta}$ is the same for both continuous and discrete cases. If the conditional distribution of the response variable is from the exponential family, for instance, the binomial or Poisson model, and the link function is canonical, then

$$\begin{aligned} \frac{\partial \ln f(\mathbf{Z} | M\boldsymbol{\delta}, \boldsymbol{\beta})}{\partial\boldsymbol{\beta}} &= X^T (\mathbf{Z} - E[\mathbf{Z} | M\boldsymbol{\delta}, \boldsymbol{\beta}]), \\ \frac{\partial^2 \ln f(\mathbf{Z} | M\boldsymbol{\delta}, \boldsymbol{\beta})}{\partial\boldsymbol{\beta}\partial\boldsymbol{\beta}^T} &= -X^T V(\mathbf{Z} | M\boldsymbol{\delta}, \boldsymbol{\beta}) X, \end{aligned} \tag{4}$$

where $V(\mathbf{Z} | M\boldsymbol{\delta}, \boldsymbol{\beta})$ is a diagonal matrix with elements whose values are the conditional variance of \mathbf{Z} .

Estimation for $\boldsymbol{\theta}$ is discussed separately for the two cases. In the continuous case $\boldsymbol{\theta} =$

(σ^2, ϕ) . For a given ϕ , the analytical derivatives in (3) with respect to σ^2 are

$$\frac{\partial \ln f(\boldsymbol{\delta}|\boldsymbol{\theta})}{\partial \sigma^2} = -\frac{q}{2\sigma^2} + \frac{1}{2(\sigma^2)^2} \boldsymbol{\delta}^T \boldsymbol{\delta}, \quad \frac{\partial^2 \ln f(\boldsymbol{\delta}|\boldsymbol{\theta})}{\partial (\sigma^2)^2} = \frac{q}{2(\sigma^2)^2} - \frac{1}{(\sigma^2)^3} \boldsymbol{\delta}^T \boldsymbol{\delta}. \quad (5)$$

The analytical derivatives with respect to ϕ , however, are not available, as the projection matrix $M = M_\phi$ is related to ϕ in a complicated fashion. Therefore, we estimate ϕ via a numerical routine. At the t^{th} iteration, we first update $(\boldsymbol{\beta}(\phi)^{(t+1)}, \sigma^2(\phi)^{(t+1)})$ conditioning on $\boldsymbol{\psi}^{(t)}$; they are plugged into the approximated Q -function $\hat{Q}(\boldsymbol{\psi}, \boldsymbol{\psi}^{(t)})$ to obtain $\hat{Q}(\phi)$. We then perform a numerical search on the neighboring values of $\phi^{(t)}$ to find $\phi^{(t+1)}$ that satisfies $\hat{Q}(\phi^{(t+1)}) > \hat{Q}(\phi^{(t)})$. In the discrete case $\boldsymbol{\theta} = \tau$. The derivatives with respect to the smoothing parameter τ are

$$\frac{\partial \ln f(\boldsymbol{\delta}|\tau)}{\partial \tau} = \frac{q}{2\tau} - \frac{1}{2} \boldsymbol{\delta}^T Q_\delta \boldsymbol{\delta}, \quad \frac{\partial^2 \ln f(\boldsymbol{\delta}|\tau)}{\partial \tau^2} = -\frac{q}{2\tau^2}.$$

The uncertainty of the estimates can be quantified by the asymptotic standard errors for the MLE, which is approximated using the observed information matrix $I(\boldsymbol{\psi}; \mathbf{Z}) = -\partial^2 / \partial \boldsymbol{\psi} \partial \boldsymbol{\psi}^T \ln L(\boldsymbol{\psi}; \mathbf{Z})$. Often it is readily obtainable from the last iteration of the maximization step if a gradient approach is used in the M-step (McLachlan and Krishnan, 2007, Sec. 4),

$$\begin{aligned} I(\boldsymbol{\psi}; \mathbf{Z}) &= \mathcal{I}_c(\boldsymbol{\psi}; \mathbf{Z}) - E [S_c(\boldsymbol{\psi}; \mathbf{Z}, \boldsymbol{\delta}) S_c^T(\boldsymbol{\psi}; \mathbf{Z}, \boldsymbol{\delta}) | \mathbf{Z}] \\ &\quad + E [S_c(\boldsymbol{\psi}; \mathbf{Z}, \boldsymbol{\delta}) | \mathbf{Z}] E [S_c^T(\boldsymbol{\psi}; \mathbf{Z}, \boldsymbol{\delta}) | \mathbf{Z}], \end{aligned} \quad (6)$$

where $\mathcal{I}_c(\boldsymbol{\psi}; \mathbf{Z}) = -Q''$ is the conditional expectation of the complete-data information matrix, and $S_c(\boldsymbol{\psi}; \mathbf{Z}, \boldsymbol{\delta})$ is the first derivative of the conditional log complete-data likelihood. The observed information matrix only need to be evaluated once at the last EM iteration with little addition computation, as the first term is a result from the EM, the second term is approximated in the last EM iteration, and the third term is zero under the MLE. The parametric bootstrap (Efron and Tibshirani, 1993) is another useful approach for obtaining standard errors of the estimates. For the parametric bootstrap, we first fit the projection-based model to the data to obtain parameter estimates. Then, multiple data sets are simulated from SGLMM. For each simulated data set, we again fit the projection-based

model. Finally, we estimate the standard errors from the point estimates.

Similar to the traditional SGLMM, the projection-based models do not have a closed form expression for the conditional expectation required in the E-step. We derive two approximation methods for the projection-based model, which results in two variants of the EM algorithm.

4.2 MCMC-EM Algorithm

We develop an automated MCMC-EM algorithm for the projection-based models, where the conditional expectations are approximated using MCMC samples. The Monte Carlo sample size at each EM iteration is selected automatically which reduces the amount of manual tuning. The E-step includes

(a) Simulation: obtain an MCMC sample $\boldsymbol{\delta}^{(t,1)}, \dots, \boldsymbol{\delta}^{(t,k_t)}$, with a sample size of k_t , from $f_{\boldsymbol{\delta}|\mathbf{Z}}(\boldsymbol{\delta}|\mathbf{Z}, \boldsymbol{\psi}^{(t)})$ under the current $\boldsymbol{\psi}^{(t)}$.

(b) Monte Carlo integration: approximate conditional expectation using average, $\hat{Q}(\boldsymbol{\psi}, \boldsymbol{\psi}^{(t)}) = \frac{1}{k_t} \sum_{k=1}^{k_t} \ln f_{\mathbf{Z},\boldsymbol{\delta}}(\mathbf{Z}, \boldsymbol{\delta}^{(t,k)}; \boldsymbol{\psi})$.

4.2.1 MCMC Sampling

Monte Carlo samples from the conditional distribution can be easily obtained using an MCMC algorithm (Robert and Casella, 2005). The projection-based models have reduced-dimensional and de-correlated random effects; this is advantageous in constructing MCMC over the traditional SGLMMs. We use the Metropolis-Hastings algorithm with a multivariate normal proposal function for sampling $\boldsymbol{\delta}$.

Several strategies are utilized for constructing an efficient MCMC algorithm. (1) We use adaptive MCMC (Roberts and Rosenthal, 2009) to avoid tedious manual tuning and to maintain desirable acceptance rate; for the $(t+1)^{th}$ EM iteration, we adjust the variance of the proposal function using $0.95 \times 2.38^2/q \times \Sigma_t + 0.05 \times (0.1)^2/q \times \mathbf{I}_q$, where Σ_t is the sample covariance of the target distribution based on the current k_t sample. (2) We initiate the MCMC using the last iteration of MCMC from the previous EM update, $\boldsymbol{\delta}^{(t+1,1)} = \boldsymbol{\delta}^{(t,k_t)}$, to obtain a good starting value. (3) We automatically adjust the Monte Carlo sample size for

each EM iteration using the ascent-based approach proposed by Caffo et al. (2005) in order to recover EM’s ascent property and allocate computing resources efficiently. A sketch of the ascent-based approach and our implementation are provided below.

4.2.2 Sample Size Selection

The Monte Carlo sample size k_t at the t^{th} EM iteration is chosen automatically such that it increase the Q -function with a high probability. Let $\Delta Q(\boldsymbol{\psi}^{(t,k_t)}, \boldsymbol{\psi}^{(t-1)}) \equiv Q(\boldsymbol{\psi}^{(t,k_t)}, \boldsymbol{\psi}^{(t-1)}) - Q(\boldsymbol{\psi}^{(t-1)}, \boldsymbol{\psi}^{(t-1)})$ be the change in the Q -function. Its approximation $\Delta \hat{Q}(\boldsymbol{\psi}^{(t,k_t)}, \boldsymbol{\psi}^{(t-1)})$, or simply $\Delta \hat{Q}$, computed from the Monte Carlo integration step, when suitably normalized, has a limiting normal distribution centered at ΔQ and a variance $\sigma_{\Delta Q}^2$. Let z_α be the $(1 - \alpha)^{\text{th}}$ percentile of a standard normal random variable z . We compute the asymptotic lower bound, $\Delta \hat{Q} - z_\alpha \text{ASE}$, where ASE denotes the asymptotic standard error estimated using batch means (Flegal et al., 2008). If the asymptotic lower bound is negative, then the increase in the Q -function is indistinguishable from zero due to a large Monte Carlo error, indicating that a larger sample size is required. Using this as a guideline, we increase sample size from k_t to $k_t + k_t/2$ until the asymptotic lower bound is positive. The required Monte Carlo sample sizes are typically small in the early EM iterations, and gradually increase as the parameter estimates get near the optimal region (Figure 2). To ensure that a large enough Monte Carlo sample is obtained at the first EM iteration to fully explore the parameter space and to estimate the correlation structure of the target distribution, we run the MCMC until the multivariate effective sample size (Gong and Flegal, 2016) is at least 10 times the dimension of the target distribution.

4.2.3 Approximate Conditional Expectations

After obtaining the MCMC samples $\boldsymbol{\delta}^{(t,k)}$, $k = 1, \dots, k_t$ from $f_{\boldsymbol{\delta}|\mathbf{Z}}(\boldsymbol{\delta}|\mathbf{Z}, \boldsymbol{\psi}^{(t)})$, the conditional expectations in (4) is approximated by

$\frac{1}{k_t} \sum_k X^T (\mathbf{Z} - E[\mathbf{Z}|M\boldsymbol{\delta}^{(t,k)}, \boldsymbol{\beta}^{(t)}])$ and $\frac{1}{k_t} \sum_k X^T V(\mathbf{Z}|M\boldsymbol{\delta}^{(t,k)}, \boldsymbol{\beta}^{(t)})X$. The conditional expectations in (5) involves computing $E[\boldsymbol{\delta}^T \boldsymbol{\delta}|\mathbf{Z}, \boldsymbol{\psi}^{(t)}]$ which is approximated by $\frac{1}{k_t} \sum_k \boldsymbol{\delta}^{(t,k)T} \boldsymbol{\delta}^{(t,k)}$.

The numerical maximization of ϕ is reduced to computing the difference

$$\begin{aligned} \hat{Q}(\phi^*) - \hat{Q}(\phi^{(t)}) &= -\frac{1}{2} \left(\sum_{i=1}^m \ln(d_{\phi^*,i}) - \sum_{i=1}^m \ln(d_{\phi,i}) \right) - \frac{1}{2\sigma^{2,(t+1)}} \\ &\quad \times \frac{1}{k_t} \sum_{k=1}^{k_t} (M\boldsymbol{\delta}^{(t,k)})^T (U_{\phi^*} D_{\phi^*}^{-1} U_{\phi^*}^T - U_{\phi} D_{\phi}^{-1} U_{\phi}^T) (M\boldsymbol{\delta}^{(t,k)}), \end{aligned} \quad (7)$$

where ϕ^* is a neighboring value of $\phi^{(t)}$. The above comparison is performed for several neighboring values, and the one with the largest increase is set to $\phi^{(t+1)}$. The major computation involved is computing the eigenvectors of R_{ϕ^*} ; performing eigendecompositions several iterations for data size up to a couple of thousands is relatively fast, and we can parallelize it for multiple ϕ using a multicore machine. If the data size is much larger than a few thousands, we can approximate the eigenvectors using a probabilistic Nyström's approximation algorithm (see supplementary materials).

4.3 Laplace Approximation EM

Laplace approximation is a fast alternative to Monte Carlo integration for approximating the conditional expectations. It is performed for every EM iteration and includes two parts:

(a) Gaussian approximation: approximate $f_{\boldsymbol{\delta}|\mathbf{Z}}(\boldsymbol{\delta}|\mathbf{Z}, \boldsymbol{\psi})$ with a Gaussian distribution $f_G(\boldsymbol{\delta}|\mathbf{Z}, \boldsymbol{\psi})$.

(b) Taylor expansion for functions of the random effects $h(\boldsymbol{\delta})$ and approximate $E_{\boldsymbol{\delta}|\mathbf{Z}}[h(\boldsymbol{\delta})|\mathbf{Z}, \boldsymbol{\psi}]$ with $E_G[\tilde{h}(\boldsymbol{\delta})|\mathbf{Z}, \boldsymbol{\psi}]$, where $\tilde{h}(\boldsymbol{\delta})$ denotes the approximation to $h(\boldsymbol{\delta})$ and the expectation is taken with respect to f_G .

4.3.1 Gaussian Approximation

For the projection-based model, the conditional density function has the form $f_{\boldsymbol{\delta}|\mathbf{Z}}(\boldsymbol{\delta}|\mathbf{Z}, \boldsymbol{\psi}) \propto \exp\{-\frac{1}{2}\boldsymbol{\delta}^T Q_{\boldsymbol{\delta}} \boldsymbol{\delta} + \sum_i \ln f_{Z_i|M\boldsymbol{\delta}}(Z_i|M\boldsymbol{\delta}, \boldsymbol{\beta})\}$. We approximate it with a Gaussian distribution whose mean is matched with the mode and variance with the inverse of the negative Hessian of $f_{\boldsymbol{\delta}|\mathbf{Z}}(\boldsymbol{\delta}|\mathbf{Z}, \boldsymbol{\psi})$ evaluated at the mode.

We first Taylor expand $\sum_i \ln f_{Z_i|M\boldsymbol{\delta}}(Z_i|M\boldsymbol{\delta}, \boldsymbol{\beta})$ to the second order around an initial guess $\boldsymbol{\delta}^{(0)}$. This will give a quadratic form in $\boldsymbol{\delta}$, for example, for count observations this becomes

$-\frac{1}{2}\boldsymbol{\delta}^T M^T D_2 M \boldsymbol{\delta} + \boldsymbol{\delta}^T M^T (Z - d_1 + D_2 H \boldsymbol{\delta}^{(0)}) + const$, where $D_2 = \text{diag}(\exp(X\boldsymbol{\beta} + M\boldsymbol{\delta})) |_{\boldsymbol{\delta}=\boldsymbol{\delta}^{(0)}}$ is an $n \times n$ diagonal matrix, $d_1 = \exp(X\boldsymbol{\beta} + M\boldsymbol{\delta}) |_{\boldsymbol{\delta}=\boldsymbol{\delta}^{(0)}}$ is an n -dimensional vector and $const$ is a constant that does not depend on $\boldsymbol{\delta}$. For Poisson observation model, D_2 and d_1 have the same elements, but this is not always the case for the exponential family; as an example, Gaussian approximation for the binary case is shown in the supplementary materials.

The conditional density function is then approximately

$$f_{\boldsymbol{\delta}|Z}(\boldsymbol{\delta}|\mathbf{Z}, \boldsymbol{\psi}) \approx \exp \left\{ -\frac{1}{2}\boldsymbol{\delta}^T (M^T D_2 M + Q_\delta) \boldsymbol{\delta} + \boldsymbol{\delta}^T M^T (Z - d_1 + D_2 M \boldsymbol{\delta}^{(0)}) \right\},$$

which has a form similar to the density function of a multivariate Normal $N(Q^{-1}b, Q^{-1})$ with $Q = M^T D_2 M + Q_\delta$ and $\mathbf{b} = M^T (Z - d_1 + D_2 M \boldsymbol{\delta}^{(0)})$. We find the mode $\boldsymbol{\delta}^*$ using Newton-Raphson by solving $\boldsymbol{\delta} = Q^{-1}\mathbf{b}$ iteratively until convergence. Once obtaining the mode, the mean and variance of the Gaussian approximation $f_G(\boldsymbol{\delta}|\mathbf{Z}, \boldsymbol{\psi})$ are $E(\boldsymbol{\delta} | \mathbf{Z}, \boldsymbol{\psi}) = \boldsymbol{\delta}^*$ and $V(\boldsymbol{\delta} | \mathbf{Z}, \boldsymbol{\psi}) = Q^{-1} |_{\boldsymbol{\delta}=\boldsymbol{\delta}^*}$, respectively.

4.3.2 Approximate Conditional Expectations

The terms to be approximated in the conditional expectations has the form

$E_{\boldsymbol{\delta}|Z} [h(X_i\boldsymbol{\beta} + M_i\boldsymbol{\delta}) | \mathbf{Z}_i, \boldsymbol{\psi}^{(t)}]$. We use $\tilde{h}(X_i\boldsymbol{\beta} + M_i\boldsymbol{\delta})$ to denote the second order Taylor expansion of $h(X_i\boldsymbol{\beta} + M_i\boldsymbol{\delta})$ around $\boldsymbol{\delta}^*$, then

$$\begin{aligned} \tilde{h}(X_i\boldsymbol{\beta} + M_i\boldsymbol{\delta}) &= h(X_i\boldsymbol{\beta} + M_i\boldsymbol{\delta}^*) + (\boldsymbol{\delta} - \boldsymbol{\delta}^*)^T (h'(X_i\boldsymbol{\beta} + M_i\boldsymbol{\delta}^*) \times M_i^T) \\ &\quad + \frac{1}{2}(\boldsymbol{\delta} - \boldsymbol{\delta}^*)^T (h''(X_i\boldsymbol{\beta} + M_i\boldsymbol{\delta}^*) \times M_i^T M_i) (\boldsymbol{\delta} - \boldsymbol{\delta}^*), \end{aligned} \tag{8}$$

where M_i is the i^{th} row of the projection matrix M , and $h'(x^*) = dh(x)/dx |_{x=x^*}$. We take the expectation of the above with respect to $f_G(\boldsymbol{\delta} | \mathbf{Z}, \boldsymbol{\psi}^{(t)})$ and obtain the following,

$$\begin{aligned}
& E_G \left[\tilde{h}(X_i\boldsymbol{\beta} + M_i\boldsymbol{\delta}) | \mathbf{Z}_i, \boldsymbol{\psi}^{(t)} \right] \\
&= h(X_i\boldsymbol{\beta} + M_i\boldsymbol{\delta}^*) + E \left[(\boldsymbol{\delta} - \boldsymbol{\delta}^*)^T | \mathbf{Z}, \boldsymbol{\psi}^{(t)} \right] \left(h'(X_i\boldsymbol{\beta} + M_i\boldsymbol{\delta}^*) \times M_i^T \right) \\
&+ \frac{1}{2} tr \left\{ E \left[(\boldsymbol{\delta} - \boldsymbol{\delta}^*)(\boldsymbol{\delta} - \boldsymbol{\delta}^*)^T | \mathbf{Z}, \boldsymbol{\psi}^{(t)} \right] \left(h''(X_i\boldsymbol{\beta} + M_i\boldsymbol{\delta}^*) \times M_i^T M_i \right) \right\} \quad (9) \\
&= h(X_i\boldsymbol{\beta} + M_i\boldsymbol{\delta}^*) + \frac{1}{2} tr \left\{ Q^{-1} \left(h''(X_i\boldsymbol{\beta} + M_i\boldsymbol{\delta}^*) \times M_i^T M_i \right) \right\}, \\
&= h(X_i\boldsymbol{\beta} + M_i\boldsymbol{\delta}^*) + \frac{1}{2} \left(h''(X_i\boldsymbol{\beta} + M_i\boldsymbol{\delta}^*) \times M_i Q^{-1} M_i^T \right).
\end{aligned}$$

The second equality holds as $E \left[(\boldsymbol{\delta} - \boldsymbol{\delta}^*)^T | \mathbf{Z}, \boldsymbol{\psi}^{(t)} \right] = 0$ and

$$E \left[(\boldsymbol{\delta} - \boldsymbol{\delta}^*)(\boldsymbol{\delta} - \boldsymbol{\delta}^*)^T | \mathbf{Z}, \boldsymbol{\psi}^{(t)} \right] = Q^{-1} |_{\boldsymbol{\delta}=\boldsymbol{\delta}^*}.$$

4.4 Rank Selection

The projection-based model is based on spatial filtering (Griffith, 2013) and principal component analysis. We can fit non-spatial generalized linear models with predictors X and synthetic spatial variables $U_m D_m^{1/2}$ for $m = 1, 2, \dots$ where the eigenvectors are computed from $R_{\phi^{(0)}}$ using an initial range value $\phi^{(0)}$. Then the rank can be selected based on variable selection criterion such as AIC. This serves as a general guideline for selecting the initial rank. Based on this, we can then fit a few models with different ranks and perform cross-validation or a likelihood ratio test to determine the final model.

4.5 Computational Benefit from the Projection-Based Models

Both the MCMC-EM and LA-EM algorithms can be used for inference for the traditional SGLMM. However, several computational challenges make it prohibitive when the data size is large. In the MCMC-EM algorithm, (1) Monte Carlo sampling from $f_{W|Z}(\mathbf{W} | \mathbf{Z}, \boldsymbol{\psi}^{(t)})$ requires manipulating a large $n \times n$ matrix, which is computationally slow even for high performance computers. (2) The random effects are also highly correlated, making it difficult to construct an efficient sampling algorithm. The reparameterization in the projection-based model replaces the original random effects \mathbf{W} with a much smaller number of new random

effects $\boldsymbol{\delta}$ that are also de-correlated, resolving the above two challenges simultaneously. Using the LA-EM algorithm to fit the traditional SGLMM requires Gaussian approximation to $f_{W|Z}$, which has the same dimension of the observations. For a relatively small number of data points, say hundreds, the Laplace approximation is fast, but as the data size grows, this will become computationally challenging. The projection-based model provides a viable solution as the dimension of random effects is reduced significantly compared to the original data size. The Gaussian approximation $f_G(\boldsymbol{\delta}|\mathbf{Z}, \boldsymbol{\psi})$ now has the same dimension as the chosen rank, which is typically much less than a hundred, therefore matrix manipulation involving its covariance matrix Q^{-1} is fast.

4.6 Spatial Prediction

SGLMMs are also often used for interpolation/prediction at unsampled locations. We describe interpolation using the projection-based models with a focus on the continuous case, since it is often less of interest for the discrete case in practice. Let $\mathcal{S}^* = \{\mathbf{s}_1^*, \dots, \mathbf{s}_{n^*}^*\}$ be a set of unsampled locations. In the projection-based model, the covariance between \mathbf{W}^* at \mathcal{S}^* and the reparameterized random effects $\widetilde{\mathbf{W}} = U_\phi D_\phi^{1/2} \boldsymbol{\delta}$ is

$$\text{cov} \left\{ \begin{pmatrix} \widetilde{\mathbf{W}} \\ \mathbf{W}^* \end{pmatrix} \right\} = \begin{pmatrix} (U_\phi D_\phi^{-1/2})^T \Sigma_\theta (U_\phi D_\phi^{-1/2}) & (U_\phi D_\phi^{-1/2})^T \Sigma_{\theta, s^*} \\ \Sigma_{\theta, s^*} (U_\phi D_\phi^{-1/2}) & \Sigma_{\theta, **} \end{pmatrix},$$

where $(U_\phi D_\phi^{-1/2})^T \Sigma_\theta (U_\phi D_\phi^{-1/2})$ is simply $\sigma^2 I_{m \times m}$. The best linear unbiased predictor (BLUP) of \mathbf{W}^* given $\widetilde{\mathbf{W}}$ is therefore $\mathbf{W}^* | \widetilde{\mathbf{W}}, \boldsymbol{\theta} \sim$

$\text{MVN}(\mu_{\mathbf{W}^* | \widetilde{\mathbf{W}}}, \Sigma_{\mathbf{W}^* | \widetilde{\mathbf{W}}})$ (Stein, 1999), where $\mu_{\mathbf{W}^* | \widetilde{\mathbf{W}}} = \frac{1}{\sigma^2} \Sigma_{\theta, s^*} (U_\phi D_\phi^{-1/2}) \widetilde{\mathbf{W}}$ and $\Sigma_{\mathbf{W}^* | \widetilde{\mathbf{W}}} = \Sigma_{\theta, **} - \frac{1}{\sigma^2} \Sigma_{\theta, s^*} (U_\phi D_\phi^{-1} U_\phi^T) \Sigma_{\theta, s^*}$. If MCMC-EM algorithm is used, to make spatial prediction we will draw from the above multivariate normal distribution for each MCMC sample of the random effects $\widetilde{\mathbf{W}} = U_\phi D_\phi^{1/2} \boldsymbol{\delta}^{(k)}, k = 1, \dots, k_t$. If LA-EM is used, then $\widetilde{\mathbf{W}}$ is approximated by $U_\phi D_\phi^{1/2} \boldsymbol{\delta}^*$, where $\boldsymbol{\delta}^*$ is the mode from the Gaussian approximation at the last EM iteration.

The prediction uncertainty from MCMC-EM is typically larger than LA-EM, as it incorporates the random effect uncertainty in prediction while LA-EM does not. However, both methods do not account for regression parameter uncertainty. If the research goal is

parameter inference or as a quick data exploratory tool, both algorithms are appropriate. If assessing spatial prediction uncertainty is the main focus, then one should keep in mind that the uncertainty from these algorithms is smaller, and therefore a fully Bayesian approach (cf. Guan and Haran, 2018) would be more appropriate.

5 Simulation Study

We study the proposed algorithms for both spatial counts and binary observations and for both continuous and discrete spatial domains. We present the results for the count data in a continuous spatial domain below. Results for count data on a lattice and binary data are similar and therefore presented in the supplementary materials.

5.1 Count Data in a Continuous Spatial Domain

We simulate $n=1400$ random effects \mathbf{W} in the unit domain $[0, 1]^2$ from the Matérn. Conditional on \mathbf{W} , we simulate Z_i from $\text{Poisson}(\mu_i)$ with $\log(\mu_i)=x_{i,1} + x_{i,2} + W_i$, where $x_{i,1}, x_{i,2}$ are the xy-coordinates of W_i . The data are generated using $\beta = (1, 1)^T$, $\nu = 1.5$, $\sigma^2 = 1$ and $\phi = 0.07$ and 0.18 . The range values correspond to effective range (defined as the distance at which the correlation is 0.05) $r = 0.2$ and 0.5 , respectively. The first 1,000 observations are located randomly in the spatial domain and are used for model fitting, while the rest are located on a 20×20 grid and are used for testing.

We suggest obtaining initial value of the regression coefficient and residual variance from fitting a non-spatial generalized linear model (GLM). It is typically difficult to obtain an estimate for the range parameter ϕ from the non-Gaussian observations; therefore, we take roughly half of the spatial domain as the initial value.

We first fit the projection-based model for two simulated data sets, each of which is simulated with different values of effective range, to investigate the parameter estimates and prediction performance of different ranks. Based on the proposed initial rank selection, the required ranks are 90 and 50 for $r = 0.2$ and 0.5 , respectively. Then we fit both algorithms using a few different ranks near the initial selection, for example, ranks 70 to 110 with an increment of 10 for the first case.

Table 1: Parameter estimates using different ranks for counts on a continuous spatial domain. Data are simulated from Matérn with $\nu = 1.5$, $\sigma_2 = 1$ and effective range of 0.2. The model fitting time are in seconds.

Rank	LA-EM					MCMC-EM				
	$\beta_1=1$	$\beta_2=1$	$\tau/\phi=13.7$	MSE	time	$\beta_1=1$	$\beta_2=1$	$\tau/\phi=13.7$	MSE	time
70	1.12	1.66	10.96	120.11	11.11	1.13	1.67	11.88	20.29	33.80
80	1.10	1.66	14.24	16.96	14.19	1.11	1.67	14.26	15.96	97.99
90	1.08	1.63	17.17	78.68	19.64	1.10	1.63	13.76	14.19	48.25
100	1.07	1.62	14.94	31.20	15.26	1.09	1.63	13.41	16.17	52.20
110	1.07	1.61	16.25	14.99	17.77	1.09	1.62	15.01	12.56	55.61

Results for $r=0.2$ is presented here because the conclusion for $r=0.5$ is similar. The initial values estimated from GLM are $\beta^{(0)} = (1.39, 1.72)^T$ and $\sigma^{2(0)} = 2.96$. For MCMC-EM, we have used $\alpha=0.15$, $\gamma=0.05$, and $\epsilon=0.001$. Parameter estimates and prediction performance are summarized in Table 1. The results suggest that rank 90 seems to be sufficient, as the parameter estimates become stable and the prediction MSE improvement decreases. We also notice that the prediction from the LA-EM algorithm consistently under-performs compared to the MCMC-EM. This suggests that the random effects estimated from Laplace approximation are not as reliable as the Monte Carlo approach. Figure 1 shows the predicted linear component in the conditional mean from the two algorithms. Table 1 also records the computational time; it takes 1-2 minutes to fit MCMC-EM and less than 20 seconds for LA-EM. These are much faster than the fully Bayesian with MCMC approach proposed in (Guan and Haran, 2018), which took roughly 4 hours for the same data size.

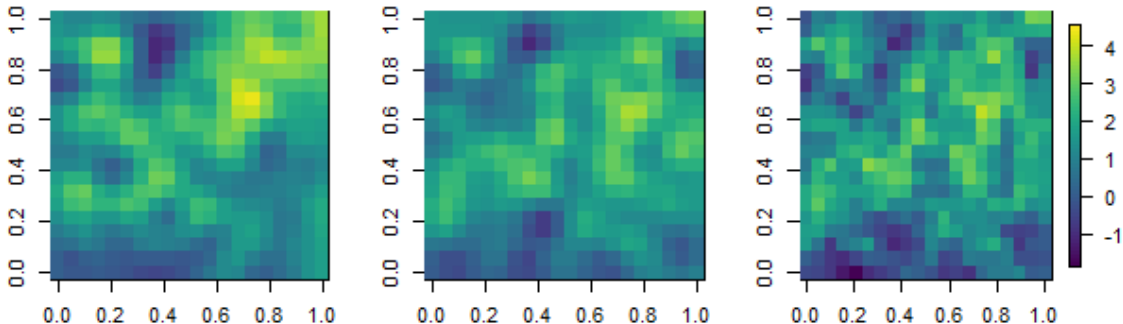


Figure 1: Predicted linear component in the conditional mean from the LA-EM (left), MCMC-EM (center) and the true (right). Data are simulated from Matérn with $\nu = 1.5$, $\sigma_2 = 1$ and effective range of 0.2.

To monitor convergence and study the robustness of the two algorithms to initial value,

we run both algorithms for a fixed number of iterations at three different starting values. We found that LA-EM algorithm is more sensitive to initial value than MCMC-EM. For the same initial values tested, MCMC-EM typically converges within 30 EM iterations, while LA-EM may diverge if the initial value is not carefully selected. For the simulated data, the initial value obtained from GLM works well for both algorithms.

Since MCMC-EM is more robust to different initial values, here we focus on illustrating the performance of MCMC-EM. Figure 2 shows the parameter estimates at each iteration from the MCMC-EM algorithm; the parameter estimates converge to the same values, regardless of starting values, all within 30 EM iterations. Figure 2 also shows the Monte Carlo sample sizes at each EM iteration; most of the simulation efforts are spent in the first and last 2-3 EM iterations. Typically, when the stopping threshold is reached (indicated by the vertical dashed line), the ascent-based MCMC-EM algorithm provides a large Monte Carlo sample. This is a desirable feature, since the last MC sample is used in subsequent analyses, for instance, for estimating the observed information matrix and spatial prediction. Finally, the integrated log-likelihood function corresponding to different starting values stabilizes as the EM iteration increases.

We conduct a simulation study with 100 replicates to study the distribution of the point estimates. Figure 3 shows the boxplots of the estimates; it appears that for both algorithms $\hat{\beta}$ are unbiased, while $\hat{\theta}$ have positive biases.

We compare the interval estimation based on the observed information matrix and bootstrap. For the latter, a bootstrap sample of 100 replicates was used to compute the confidence intervals for each simulated data set. The coverages based on the observed information matrix are around 15%, much lower than the nominal rate 95%, whereas the coverages based on bootstrap are near 95%, because the confidence intervals (CIs) provided by the observed information matrix is much narrower than the ones from bootstrap and therefore missed the true values.

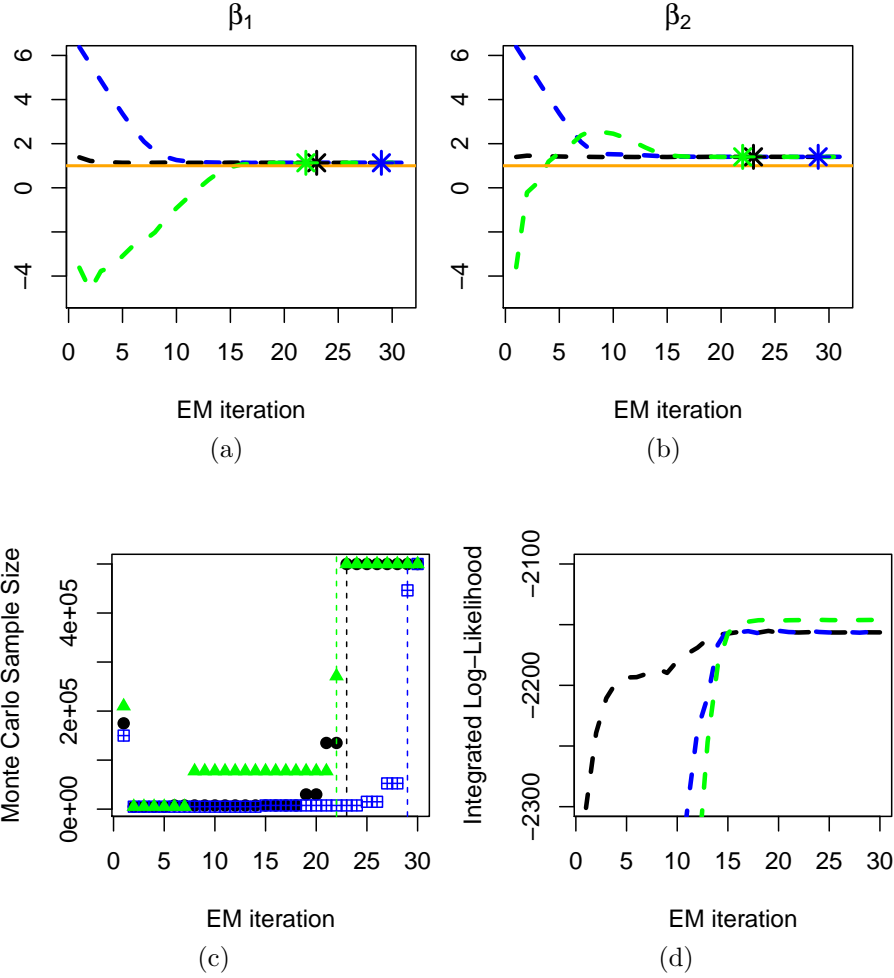


Figure 2: Parameter estimates from MCMC-EM with different starting values (a-b). Asterisk indicates the stopping threshold is reached. Monte Carlo sample size (c) is adjusted automatically, with increasing simulation efforts as EM iteration increases. We typically obtain a large MC sample when the algorithm stops; vertical line indicates the stopping threshold is reached. Integrated log-likelihood function (d) corresponding to different starting values stabilize as EM iteration increases.

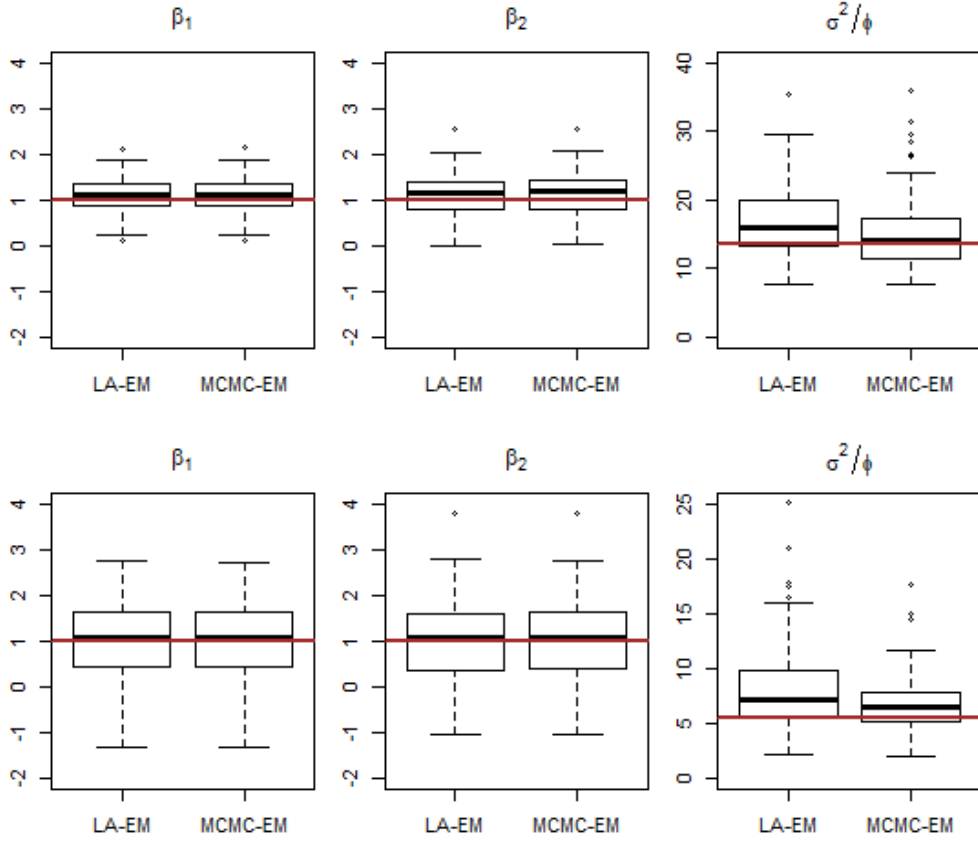


Figure 3: Distributions of the estimates from both LA-EM and MCMC-EM algorithm for spatial counts in continuous spatial domain. Data are simulated from Matérn with $\nu = 1.5$, $\sigma_2 = 1$ and effective range of 0.2 in the top panel or effective range of 0.5 in the bottom panel. It seems that $\hat{\beta}$ are unbiased while $\hat{\theta}$ has positive biases.

6 Data Analysis

6.1 US Infant Mortality Data

We fit the projection-based model for the county-level US infant mortality from 2002 to 2004, a data set analyzed in Hughes and Haran (2013) under a Bayesian approach. The response variable is the 3-year average number of infant deaths before the first birthday, and the predictors are the rate of low birth weight (low), the percentage of black residents (black), the percentage of Hispanic residents (Hisp), a measure of income inequality (the Gini coefficient proposed by Gini, 1921), a composite score of social affluence (aff, proposed by Yang et al., 2009) and residential stability (stab, an average z-score of two variables). Similar to Hughes and Haran (2013), we use the 3-year average number of live births as an offset to adjust for the population difference in these counties. The point and interval estimates from the maximum likelihood inference using MCMC-EM method are shown in the supplementary materials; our results are very comparable to the ones from the Bayesian inference with MCMC in Hughes and Haran (2013).

6.2 Forest/Non-forest Land Type Data

The land type of a region, whether it is covered by forest or non-forest, is often of interest for economic and environmental reasons. Spatial regression can be used for assessing the relationship between forest/nonforest binary response and potential covariates while accounting for the residual spatial dependence. We use a data set analyzed in Berrett and Calder (2016). The response variable is 2005 Land Cover Type Yearly Level 3 Global 500 m (MOD12Q1 and MCD12Q1) data from Moderate Resolution Imaging Spectroradiometer (MODIS); the MODIS land cover data are categorized into two types, forest and nonforest. The study region is a 24×24 regular grid between 17° - 19° N and 98° - 100° E, covering a portion of northwestern Thailand and a small part of Myanmar. We randomly sample 450 out of 576 grid cells for training, and test on the remaining for model validation. In our analysis, the observations are modeled using a Gaussian random field latent process with coordinates taken to be the centroid of the grid cells. The covariates considered are elevation, distance

to the coast, distance to nearest big city, and distance to the nearest major road.

We fit the projection-based model using the MCMC-EM algorithm using rank 70. Based on our analysis, it appears that higher elevation, longer distance to the coast and road are associated with higher forest coverage for this area. The point and interval estimates from the maximum likelihood inference using MCMC-EM is presented in the supplementary materials.

7 Summary

We have proposed two variants of the EM algorithm that allow us to carry out maximum likelihood inference for SGLMMs. These algorithms take advantage of recent developments in dimension reduction of latent variables using projection methods (Hughes and Haran, 2013; Guan and Haran, 2018). Our algorithms are computationally efficient and allow us to do maximum likelihood inference for problems where it was previously computationally prohibitive. While our goal is to do maximum likelihood inference, we also find that the algorithms are faster than corresponding MCMC-based Bayesian inference procedures in the continuous domain setting, and are comparable in speed in the discrete domain setting. Parameter estimates seem to converge quickly for both algorithms, however LA-EM is less robust to initial values and may fail when initial values are far from the MLE. We recommend using initial values estimated from a fitted GLM, which worked well for both algorithms in our simulation study.

Maximum likelihood inference has not been as popular as Bayesian inference for SGLMMs, at least in part because of computational issues. We hope that the methodology we develop here, which addresses inference for a large class of models, including both latent Gaussian process and Gaussian Markov random field models, will allow researchers to routinely fit SGLMMs using maximum likelihood inference. We do not believe that this will entirely replace Bayesian approaches as Bayesian models allow for a greater range of flexibility in terms of adding additional hierarchies, handling missing data, and combining information from multiple variables routinely. However, for a wide range of problems, the class of SGLMMs for which we have developed a computationally efficient set of methods here, maximum like-

likelihood inference may now be a convenient and viable option. Furthermore, because the work on practical EM algorithms for SGLMMs and other models with high-dimensional dependent latent variables has been somewhat limited, we hope that our work suggests directions for future work on scalable EM-type algorithms for such problems.

Supplementary Materials Contain eigencomponent approximation, Laplace approximation for binary data, stopping criterion, simulation study results for count data on a lattice and binary data, and application results.

Acknowledgements We thank Dr. Candace Berrett for sharing the land type data. This work was partially supported by NSF through DMS-1418090, DMS-1638521 and GEO1240507, and NIH through R01GM123007.

Supplementary materials to “Fast expectation-maximization algorithms for spatial generalized linear mixed models” by Guan and Haran

S.1 Approximating Eigencomponents

Fitting projection-based models for the continuous case requires eigendecomposition on R_ϕ for every ϕ update. When the number of data points is large, exact eigendecomposition is infeasible; we propose to approximate the principal components using a probabilistic version of Nyström’s method. Probabilistic algorithms have been increasing in popularity for fast matrix decompositions (see Halko et al., 2011, for a summary of algorithms). Banerjee et al. (2013) proposed using them for approximating covariance matrices in the linear Gaussian process regression setting. This was extended in Guan and Haran (2018) to approximate eigencomponents for SGLMMs. Here, we provide details of the probabilistic algorithm used by Guan and Haran (2018) which combines ideas from random-projection with Nyström’s method.

We first introduce the deterministic Nystöm’s method (Williams and Seeger, 2001). Let K denote an $n \times n$ positive semi-definite matrix and Φ an $n \times m$ truncation matrix by permuting the rows of $[I_{m \times m}, 0_{m \times (n-m)}]^T$. The Nystöm’s method partitions K into four blocks, $\begin{bmatrix} K_{11} & K_{12} \\ K_{21} & K_{22} \end{bmatrix}$, by sub-sampling its columns and rows, and letting $K_{11} = \Phi^T K \Phi$. Then, it performs an exact decomposition on the $m \times m$ sub-matrix K_{11} to obtain its eigenvectors V_{11} and eigenvalues $\Lambda_{11} = \text{diag}(\lambda_{11,1}, \dots, \lambda_{11,m})$. Finally, it maps the low-dimensional eigenvectors V_{11} to high dimension via $\sqrt{\frac{m}{n}}[K\Phi][V_{11}\Lambda_{11}^{-1}]$ (Drineas and Mahoney, 2005).

In the probabilistic algorithm, we replace the truncation matrix Φ with $K^a \Omega$, where Ω is an $n \times (m+l)$ random matrix with $\Omega_{ij} \sim N\left(0, 1/\sqrt{(m+l)}\right)$, and $a = 0, 1$, or 2 is a small non-negative integer to improve approximation (see Guan and Haran, 2018, for a discussion on a); l is an oversampling factor to reduce approximation error (Halko et al., 2011). Here, we take $l = m$ ($n > m+l$), and $a = 1$. The eigenvectors approximated using the

Nystöm's method are not guaranteed to be orthogonal; therefore, we take an additional step to orthogonalize the column vectors, i.e. we will use the first m columns of the left singular vectors of $[K\Phi][V_{11}\Lambda_{11}^{-1/2}]$ as the final approximation to the eigenvectors. The algorithm is summarized in Algorithm 1.

Algorithm 1 Probabilistic Nyström's Approximation

This algorithm approximates the leading m eigencomponents of an $n \times n$ positive semi-definite matrix K , combining random projection and the Nyström's method.

1. Low dimensional projection from $R^{n \times n}$ to $R^{n \times (m+l)}$:
Form $\Phi = K\Omega$, where $\Omega_{ij} \sim N(0, 1/\sqrt{(m+l)})$.
 2. Nyström's method to approximate eigencomponents:
Form $K_1 = \Phi^T K \Phi$
SVD for K_1 : $V_{11}\Lambda_{11}V_{11}^T$
Form Nyström extension $C = [K\Phi][V_{11}\Lambda_{11}^{-1/2}]$
SVD for C : UDV^T
 3. Take the first m columns of U , and the first m diagonal elements of D^2 as our approximation to the leading m eigencomponents of K
-

S.2 Laplace Approximation for Binary Data

For binary data with a logit link function, the Taylor expansion for the logarithm of the incomplete-data likelihood is derived here,

$$\begin{aligned}
\sum_i \ln f_{Z_i|M\delta}(Z_i|M\delta, \beta) &= Z^T(X\beta + M\delta) - \sum_i \log(1 + \exp(X\beta + M\delta)) \\
&\approx Z^T(X\beta + M\delta^{(0)}) - \sum_i \log(1 + \exp(X\beta + M\delta^{(0)})) \\
&\quad + (\delta - \delta^{(0)})^T \left[\sum_i \frac{\partial}{\partial \delta} \ln f_{Z_i|M\delta}(Z_i|M\delta, \beta) \right]_{\delta=\delta^{(0)}} \\
&\quad + \frac{1}{2}(\delta - \delta^{(0)})^T \left[\sum_i \frac{\partial^2}{\partial \delta \partial \delta^T} \ln f_{Z_i|M\delta}(Z_i|M\delta, \beta) \right]_{\delta=\delta^{(0)}} (\delta - \delta^{(0)})^T \\
&= -\frac{1}{2}\delta^T M^T D_2 M \delta + \delta^T M^T (Z - d_1 + D_2 H \delta^{(0)}) + const.,
\end{aligned}$$

where $D_2 = \text{diag}(\frac{\exp(X\beta + M\delta)}{(1 + \exp(X\beta + M\delta))^2}) |_{\delta = \delta^{(0)}}$ is an $n \times n$ diagonal matrix, $d_1 = \frac{\exp(X\beta + M\delta)}{1 + \exp(X\beta + M\delta)} |_{\delta = \delta^{(0)}}$ is an n -dimensional vector and $const$ is a constant that does not depend on δ .

S.3 Stopping Criterion

For MCMC-EM algorithm we use a stopping rule similar to the framework of determining Monte Carlo sample sizes based on the ascent-based approach (Caffo et al., 2005). We stop the algorithm when $\Delta \hat{Q}$ is less than ϵ with a high probability, that is, when the asymptotic upper bound $\Delta \hat{Q} + z_\gamma ASE < \epsilon$. This indicates that the integrated log-likelihood evaluated at the current estimates $\hat{Q}(\psi^{(t)}, \psi^{(t-1)})$ stabilizes. Other standard stopping rules (McLachlan and Krishnan, 2007), for example, stopping when the absolute change in estimates is small, could be used as alternatives or combined stopping criterion; we see, in our simulation study that these make little difference to how efficiently the algorithm runs. For Laplace approximation EM algorithm, we stop the EM updates when the absolute change in estimates is less than 0.001.

S.4 Count Data on a Lattice

We simulate $n=900$ random effects on a 30×30 grid from $N(\mathbf{0}, 3Q_\delta^{-1})$; here, we follow the simulation study in Hughes and Haran (2013) and use the first 400 eigenvectors to simulate the data, i.e. $\dim(\delta) = 400$ and M is 900×400 . We then simulate count observations from $\text{Poisson}(\mu_i)$, where $\log(\mu_i) = x_{i,1} + x_{i,2} + W_i$ and $x_{i,1}, x_{i,2}$ are the xy -coordinates of the vertices.

An initial rank of 80 is selected, then we fit the projection-based model using rank 60 to 100 with an increment of 10. Parameter estimates and computational time are summarized in Table 2; the parameter estimates are similar among the compared ranks and it appears that rank 70 or 80 is sufficient. We again study the convergence and robustness of both algorithms by starting at different initial values; the result here is similar to the continuous case, and therefore not shown.

We then conduct a simulation study with 100 replicates. The distributions of the point

Table 2: Parameter estimates and computational time (in seconds) from LA-EM and MCMC-EM algorithms for Poisson data on a lattice.

Rank	LA-EM				MCMC-EM			
	$\beta_1=1$	$\beta_2=1$	$\tau=3$	time	$\beta_1=1$	$\beta_2=1$	$\tau=3$	time
60	1.04	0.96	1.75	1.01	1.05	0.96	2.34	27.41
70	1.03	0.95	1.67	1.17	1.03	0.97	2.34	25.69
80	1.03	0.94	1.65	1.39	1.05	0.96	2.63	42.08
90	1.03	0.94	1.68	1.51	1.04	0.96	2.51	31.85
100	1.03	0.94	1.70	1.52	1.03	0.96	2.56	41.64

estimates are shown in Figure 4. The point estimates are distributed more tightly around the true value, because in our simulation of the data, we have restricted the random effects to be orthogonal to the fixed effects (no spatial confounding). This is what we typically see for both of the continuous and lattice cases — when there is confounding, the distributions of point estimates have larger variability, and when confounding is not an issue, the point estimates center closely to the true values. The coverages based on the observed information matrix and bootstrap are also compared. It appears that bootstrap provides better coverage, near 93% for regression parameters, but lower coverage (near 65%) is found for the variance parameter.

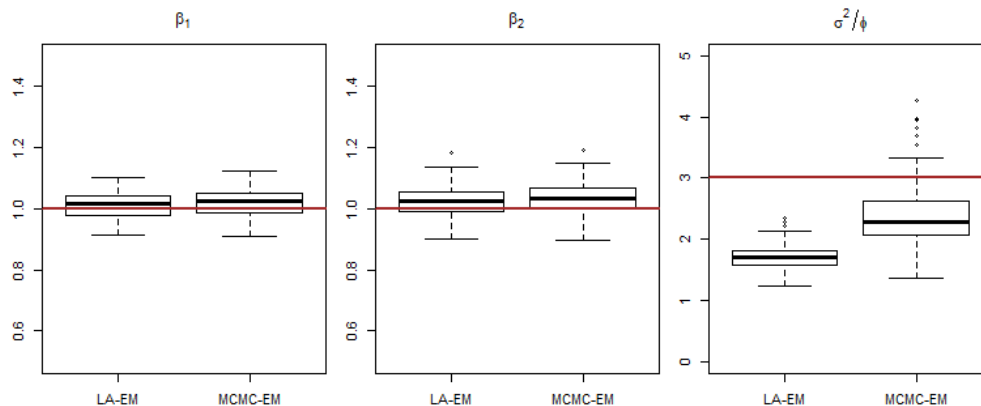


Figure 4: Distributions of the estimates from both LA-EM and MCMC-EM algorithm for count data on a lattice. It seems that $\hat{\beta}$ are unbiased and tightly center around the true value while $\hat{\theta}$ has negative biases.

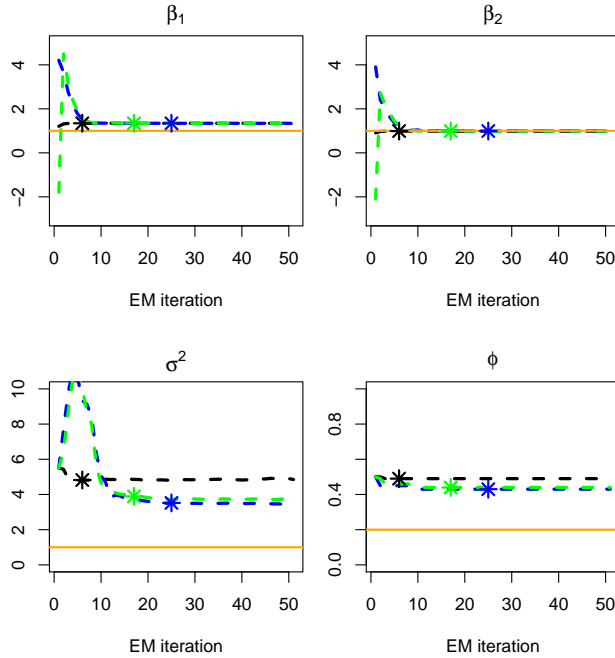


Figure 5: Parameter estimates with different starting values converge within a few iterations.

S.5 Simulation Study Results for Binary Data

Here we present the simulation study results for binary observations in a continuous domain. We first simulate $n=1400$ random effects in unit domain similar to the count data, we then simulate binary observations Z_i from $\text{Bernoulli}(p_i)$ using the logit link function, $\log\left(\frac{p}{1-p}\right)=x_{i,1} + x_{i,2} + W_i$, where $x_{i,1}, x_{i,2}$ are the xy-coordinates of W_i . The first 1000 observations, randomly located in the unit domain, are used for model fitting; the last 400 observations, on a 20×20 grid, are used for testing. Our analyses using the projection-based model have similar results as the count data. Figure 5 shows the parameter estimates. Figure 6 shows the Monte Carlo sample size and integrated log-likelihood function. Figure 7 shows the distribution of parameter estimates. Table 3 shows the inference results using different ranks.

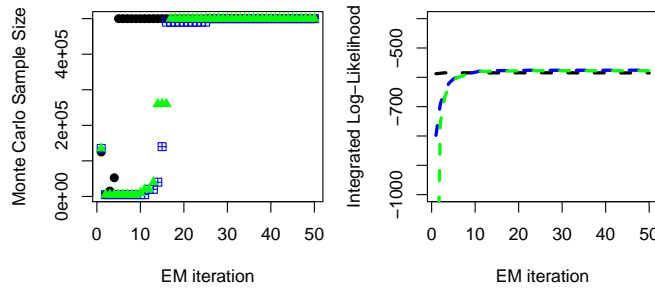


Figure 6: Monte Carlo sample size is adjusted automatic, with increasing simulation efforts as EM iteration increases (left). Integrated log-likelihood function with different starting values (right)

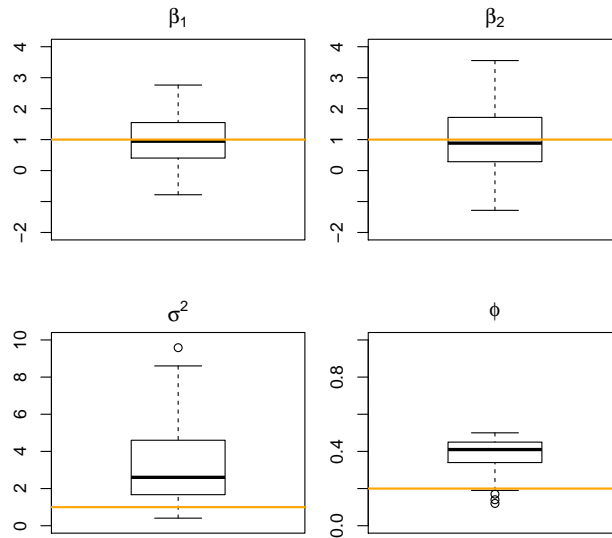


Figure 7: Distributions of point estimates. Point estimates for regression parameters center around the true value. Point estimates for covariance parameters seem to have a positive bias.

Table 3: Results for simulated binary data in continuous domain

Dimension	β_1	CI(β_1)	β_2	CI(β_2)	σ_2	CI(σ_2)	ϕ	CI(ϕ)
25	1.343	(0.947,1.738)	0.992	(0.613,1.37)	4.672	(-0.665,10.009)	0.46	—
50	1.344	(0.949,1.739)	0.989	(0.612,1.366)	4.822	(-0.366,10.009)	0.49	—
75	1.347	(0.952,1.743)	0.991	(0.613,1.37)	5.214	(-0.908,11.335)	0.49	—
100	1.344	(0.928,1.713)	0.988	(0.598,1.348)	5.116	(-0.87,9.349)	0.5	—

Table 4: Results of fitting model with rank 50 to the infant mortality data

Predictor	Parameter	Estimate	CI
Intercept	β_0	-5.423	(-5.609,-5.238)
Low birth weight	β_1	8.779	(7.521,10.037)
Black	β_2	0.004	(0.003,0.006)
Hisp	β_3	-0.004	(-0.005,-0.003)
Gini	β_4	-0.568	(-1.001,-0.136)
aff	β_5	-0.077	(-0.089,-0.065)
stab	β_6	-0.029	(-0.044,-0.015)
–	τ	7.939	(2.556,13.323)

Table 5: Results of fitting model to the land type data using rank 70.

Predictor	Parameter	Estimate	CI
Intercept	β_0	-14.213	(-20.277, -8.149)
Elevation	β_1	3.173	(1.845, 4.501)
Dist to Coast	β_2	1.234	(0.562,1.906)
Dist to City	β_3	-0.382	(-1.520,0.756)
Dist to Road	β_4	13.229	(9.961,16.497)
–	σ^2	7.939	(1.031,14.847)

S.6 Tables for Data Applications

Table 4 shows the point and interval estimates from the maximum likelihood inference using MCMC-EM for the infant mortality data, while Table 5 shows the results for the land type data.

References

- Banerjee, A., Dunson, D. B., and Tokdar, S. T. (2013). Efficient Gaussian process regression for large datasets. *Biometrika*, 100(1):75–89.
- Banerjee, S., Carlin, B., and Gelfand, A. (2014). *Hierarchical Modeling and Analysis for Spatial Data*. CRC Press.
- Banerjee, S., Gelfand, A. E., Finley, A. O., and Sang, H. (2008). Gaussian predictive process models for large spatial data sets. *Journal of the Royal Statistical Society: Series B (Statistical Methodology)*, 70(4):825–848.
- Berrett, C. and Calder, C. A. (2016). Bayesian spatial binary classification. *Spatial Statistics*, 16:72 – 102.
- Besag, J., York, J., and Mollié, A. (1991). Bayesian image restoration, with two applications in spatial statistics. *Annals of the Institute of Statistical Mathematics*, 43(1):1–20.
- Bonat, W. H. and Ribeiro, P. J. (2016). Practical likelihood analysis for spatial generalized linear mixed models. *Environmetrics*, 27(2):83–89.
- Caffo, B., Jank, W., and Jones, G. L. (2005). Ascent-based Monte Carlo expectation–maximization. *Journal of the Royal Statistical Society: Series B (Statistical Methodology)*, 67(2):235–251.
- Christensen, O. F. (2004). Monte Carlo maximum likelihood in model-based geostatistics. *Journal of Computational and Graphical Statistics*, 13(3):702–718.
- Christensen, O. F., Roberts, G. O., and Sköld, M. (2006). Robust Markov chain Monte Carlo methods for spatial generalized linear mixed models. *Journal of Computational and Graphical Statistics*, 15(1):1–17.
- Christensen, O. F. and Waagepetersen, R. (2002). Bayesian prediction of spatial count data using generalized linear mixed models. *Biometrics*, 58(2):280–286.
- Diggle, P. J., Tawn, J. A., and Moyeed, R. A. (1998). *Journal of the Royal Statistical Society: Series C (Applied Statistics)*, 47(3):299–350.
- Drineas, P. and Mahoney, M. W. (2005). On the Nyström method for approximating a Gram matrix for improved kernel-based learning. *Journal of Machine Learning Research*, 6(Dec):2153–2175.
- Efron, B. and Tibshirani, R. (1993). *An Introduction to the Bootstrap*. Taylor & Francis.
- Flegal, J. M., Haran, M., and Jones, G. L. (2008). Markov chain Monte Carlo: Can we trust the third significant figure? *Statistical Science*, pages 250–260.
- Gong, L. and Flegal, J. M. (2016). A practical sequential stopping rule for high-dimensional Markov chain Monte Carlo. *Journal of Computational and Graphical Statistics*, 25(3):684–700.

- Griffith, D. A. (2013). *Spatial autocorrelation and spatial filtering: Gaining understanding through theory and scientific visualization*. Springer.
- Guan, Y. and Haran, M. (2018). A computationally efficient projection-based approach for spatial generalized linear mixed models. *Journal of Computational and Graphical Statistics*, 27(4):701–714.
- Halko, N., Martinsson, P.-G., and Tropp, J. A. (2011). Finding structure with randomness: Probabilistic algorithms for constructing approximate matrix decompositions. *SIAM review*, 53(2):217–288.
- Hanks, E. M., Schliep, E. M., Hooten, M. B., and Hoeting, J. A. (2015). Restricted spatial regression in practice: geostatistical models, confounding, and robustness under model misspecification. *Environmetrics*, 26(4):243–254.
- Haran, M. (2011). Gaussian random field models for spatial data. In *Markov chain Monte Carlo Handbook*, pages 449–478. CRC Press.
- Haran, M., Hodges, J. S., and Carlin, B. P. (2003). Accelerating computation in Markov random field models for spatial data via structured MCMC. *Journal of Computational and Graphical Statistics*, 12:249–264.
- Hodges, J. S. and Reich, B. J. (2010). Adding spatially-correlated errors can mess up the fixed effect you love. *The American Statistician*, 64(4):325–334.
- Hughes, J. and Haran, M. (2013). Dimension reduction and alleviation of confounding for spatial generalized linear mixed models. *Journal of the Royal Statistical Society: Series B (Statistical Methodology)*, 75(1):139–159.
- Lange, K. (1995). A gradient algorithm locally equivalent to the EM algorithm. *Journal of the Royal Statistical Society: Series B (Methodological)*, pages 425–437.
- Lindgren, F., Rue, H., and Lindstrom, J. (2011). An explicit link between Gaussian fields and Gaussian Markov random fields: the stochastic partial differential equation approach. *Journal of the Royal Statistical Society: Series B (Statistical Methodology)*, 73(4):423–498.
- McLachlan, G. and Krishnan, T. (2007). *The EM Algorithm and Extensions*, volume 382. Wiley.
- Park, J. and Haran, M. (2020). Reduced-dimensional monte carlo maximum likelihood for latent gaussian random field models. *Journal of Computational and Graphical Statistics*, 0(0):1–15.
- Reich, B. J., Hodges, J. S., and Zadnik, V. (2006). Effects of residual smoothing on the posterior of the fixed effects in disease-mapping models. *Biometrics*, 62(4):1197–1206.
- Robert, C. P. and Casella, G. (2005). *Monte Carlo Statistical Methods*. Springer.
- Roberts, G. O. and Rosenthal, J. S. (2009). Examples of adaptive MCMC. *Journal of Computational and Graphical Statistics*, 18(2):349–367.

- Rue, H. and Held, L. (2005). *Gaussian Markov random fields: theory and applications*. CRC Press.
- Rue, H., Martino, S., and Chopin, N. (2009). Approximate Bayesian inference for latent Gaussian models by using integrated nested Laplace approximations. *Journal of the royal statistical society: Series b (statistical methodology)*, 71(2):319–392.
- Sengupta, A. and Cressie, N. (2013a). Empirical hierarchical modelling for count data using the spatial random effects model. *Spatial Economic Analysis*, 8(3):389–418.
- Sengupta, A. and Cressie, N. (2013b). Hierarchical statistical modeling of big spatial datasets using the exponential family of distributions. *Spatial Statistics*, 4:14 – 44.
- Stein, M. (1999). *Interpolation of Spatial Data: Some Theory for Kriging*. Springer.
- Williams, C. and Seeger, M. (2001). Using the Nyström method to speed up kernel machines. In *Advances in Neural Information Processing Systems 13*, pages 682–688. MIT Press.
- Wu, C. F. J. (1983). On the convergence properties of the EM algorithm. *The Annals of Statistics*, 11(1):95–103.
- Zhang, H. (2002). On estimation and prediction for spatial generalized linear mixed models. *Biometrics*, 58(1):129–136.
- Zilber, D. and Katzfuss, M. (2021). Vecchia–laplace approximations of generalized gaussian processes for big non-gaussian spatial data. *Computational Statistics & Data Analysis*, 153:107081.